RSC Advances

RSC Publishing

PAPER

View Article Online
View Journal | View Issue

Cite this: *RSC Adv.*, 2013, **3**, 21558

Facile synthesis of $Co_2P_2O_7$ nanorods as a promising pseudocapacitive material towards high-performance electrochemical capacitors†

Linrui Hou,*[a] Lin Lian,[a] Diankai Li,[a] Jingdong Lin,*[b] Gang Pan,[ac] Longhai Zhang,[a] Xiaogang Zhang,[c] Qingan Zhang[a] and Changzhou Yuan*[a]

Received 15th March 2013
Accepted 5th September 2013

DOI: 10.1039/c3ra41257a

www.rsc.org/advances

In the present work, we developed an efficient one-step template-free strategy to fabricate intriguing one-dimensional (1D) $Co_2P_2O_7$ nanorods (NRs) at room temperature, and utilized the unique monoclinic $Co_2P_2O_7$ NRs as an excellent electrode material for high-performance pseudocapacitors using 3 M KOH as an electrolyte. Strikingly, the as-synthesized 1D $Co_2P_2O_7$ NR electrode delivered a specific capacitance (SC) of 483 F g^{-1} at 1 A g^{-1}, and even at 402 F g^{-1} a high current loading of 10 A g^{-1}. And the SC retention of ~90% over continuous 3000 charge–discharge cycles at a current density of 6 A g^{-1}confirmed its stable long-term cycling ability at high current density. More significantly, the underlying electrochemical energy-storage mechanism of the $Co_2P_2O_7$ NR electrode in alkaline KOH aqueous solution was tentatively proposed. And the appealing strategy was proposed for future exploration and development of other low-cost pseudocapacitive materials for next-generation ECs.

Introduction

Electrochemical capacitors (ECs), also known as supercapacitors, are currently attracting increasing attention because of their appealing ability to deliver greater power density and longer cycling behavior than conventional rechargeable batteries, and energy density higher by orders of magnitude than common dielectric capacitors.[1–3] It is well established that the capacitance of ECs mainly arises from surface reaction of electroactive materials, including surface charge separation at the electrode/electrolyte interfaces (*i.e.*, electrochemical double layered capacitive behavior) as described by the Gouy–Chapman–Stern–Grahame (GCSG) mode, and surface electrochemical redox reactions (*i.e.*, pseudocapacitive behavior) on and/or near the electrode surfaces at certain potentials.[1–3] Accordingly, ECs are commonly categorized as electrical double-layer capacitors (EDLCs) and pseudocapacitors based on energy storage mechanisms. In fact, pseudocapacitors have even higher specific capacitance (SC) than conventional EDLCs due to their fast and reversible Faradaic redox reactions, therefore many efforts, including ours in this work, have been focused on further enhancing the electrochemical performance of pseudocapacitors, particularly, by choosing and rationally designing some appropriate electrode materials.

Among these typical pseudocapacitive materials, hydrous ruthenium oxide ($RuO_2 \cdot xH_2O$) enjoys a place of pride as a state-of-the-art electroactive material for pseudocapacitors, thanks to its highly reversible redox reactions, large SC, wide electrochemical window, *etc.*,[4,5] unfortunately, the high cost and serious toxicity greatly limit its extensive commercial attractiveness for ECs application. Thereby, numerous researches have been devoted to explore and develop alternative low-cost and environmentally-benign electroactive materials with favorable capacitive characteristics meanwhile. Recently, interesting pyrophosphates with excellent energy-storage applications have been greatly investigated.[6–8] In particular, Zheng and co-authors synthesized micro-/nano-structured $Mn_2P_2O_7$, and studied its electrochemical capacitance as an pseudocapacitive electrode in 1 M Na_2SO_4 solution.[6] Although the SC of the emerging $Mn_2P_2O_7$ is just as little as ~30 F g^{-1}, this pioneer work unambiguously opens up a new pathway to identify other pyrophosphates of bivalent metals with a general formula $M_2P_2O_7$ (M = Co, Ni, *etc.*) with the expectation of performing as promising pseudocapacitive candidates for advanced ECs. Recently, Pang and co-workers prepared dicobalt pyrophosphate ($Co_2P_2O_7$) nano/micro-structures through calcination of the $NH_4CoPO_4 \cdot H_2O$ precursors at a high temperature of 500 °C, and the electrochemical capacitance of the unique $Co_2P_2O_7$ electrode was also investigated.[9,10] Nevertheless, further exploration of easy one-step synthesis of electroactive $Co_2P_2O_7$ with

[a]*School of materials Science & Engineering, Anhui University of technology, Ma'anshan, 243002, P. R. China. E-mail: houlr629@163.com; ayuancz@163.com*

[b]*Department of Chemistry, College of Chemistry and Chemical Engineering, Xiamen University, Xiamen, 361005, P. R. China. E-mail: jdlin@xmu.edu.sg*

[c]*College of Material Science and Engineering, Nanjing University of Aeronautics and Astronautics, Nanjing, 210016, P. R. China*

† Electronic supplementary information (ESI) available: The detailed synthesis condition and materials characterization. See DOI: 10.1039/c3ra41257a

the absence of high-temperature procedure for high-performance ECs is of great significance for its wide application. Moreover, one-dimensional (1D) nano-structured electrodes are known to possess great potential ECs application due to their convenient transport pathways both for electrons and ions.[11,12]

Based on the above consideration and inspiration, in the work, we developed a simple yet efficient one-step strategy to fabricate novel 1D $Co_2P_2O_7$ nanorods (denoted as $Co_2P_2O_7$ NRs) without any templates and high-temperature calcination applied during the synthesis, and then applied the unique monoclinic $Co_2P_2O_7$ containing CoO_6 coordination octahedron and P_2O_7 groups (Fig. 1a) as an electroactive material for high-performance pseudocapacitors using 3 M KOH aqueous solution as an electrolyte, although its magnetic and microwave absorption properties have been greatly reported.[13,14] Impressively, the as-fabricated 1D $Co_2P_2O_7$ NRs delivered high SCs and desirable electrochemical stability at large current densities. More importantly, the underlying insights into the electrochemical energy-storage mechanism of the 1D $Co_2P_2O_7$ NR electrode in alkaline KOH aqueous solution were further tentatively proposed.

Experimental section

Synthesis of 1D $Co_2P_2O_7$ NRs

The sodium hydrogen phosphate hydrate was purchased and calcinated at 210 °C in an electric oven for 16 h. Then, the obtained white powder (1.8 g) was further dissolved in 45 mL of water solution with 2 g of CH_3COONH_4. Then, 7.5 mL of $Co(OOCCH_3)_2 \cdot 4H_2O$ solution (0.33 M) was added dropwise into the above solution with a pH = 4.14 at a rate of 1 mL min^{-1}. After stirred for another 8 h, the pH of the mixture reached 5.56. And the precipitate was isolated by centrifugation and light purple solid powder of $Co_2P_2O_7$ was obtained after drying the sample at 100 °C in an oven. For comparison, another $Co_2P_2O_7$ sample was prepared without the use of CH_3COONH_4 during the synthetic procedure.

Materials characterization

The samples were examined by powder X-ray diffraction (XRD) (Max 18 XCE, Japan) using a Cu Kα source ($\lambda = 0.154056$ nm) at a scanning speed of 3° min^{-1} over a 2θ range of 10–80°. The morphologies and structures were observed with field-emission scanning electron microscopy (FESEM, JEOL-6300F, 15 kV), and transmission electron microscope (TEM) and high-resolution TEM (HRTEM) capable of energy dispersive X-ray analysis (EDXA), and selected area electron diffraction (SAED) (JEOL JEM 2100 system operating at 200 kV).

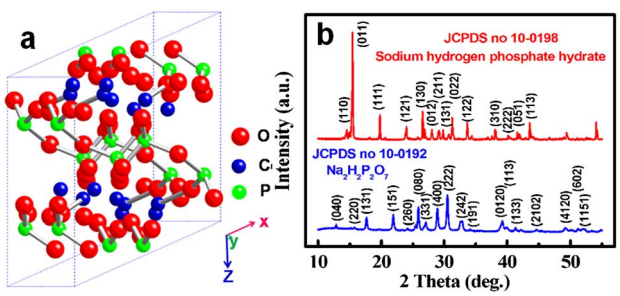

Fig. 1 Crystallographic structure of monoclinic $Co_2P_2O_7$ (a), and (b) typical XRD patterns of the sodium hydrogen phosphate hydrate ($NaH_2PO_4 \cdot 2H_2O$), and the as-obtained $Na_2H_2P_2O_7$ as indicated.

Electrochemical tests

The working electrode was prepared with the electroactive material $Co_2P_2O_7$, acetylene black (AB) and polytetrafluoroethylene (PTFE) in a weight ratio of 8 : 1.5 : 0.5. A small amount of water was then added to make more homogeneous mixture, which was pressed on nickel foam with a surface area of 1 cm^2 ($\sim 10^7$ Pa) for following electrochemical tests by cyclic voltammetry (CV), chronopotentiometry (CP) and electrochemical impedance spectroscopy (EIS) measurements performed with a IVIUM electrochemical workstation (The Netherlands). The sinusoidal excitation voltage applied during the EIS measurement was 5 mV with a frequency range between 10^5 and 10^{-2} Hz. All experiments were carried out in a three-electrode cell with a working electrode, a platinum plate counter electrode (1 cm^2) and a saturated calomel electrode (SCE) reference electrode at RT. The electrolyte used here was 3 M KOH aqueous solution. The cycling performance was carried out with a CT2001D tester (Wuhan, China). The SCs of the $Co_2P_2O_7$ electrodes can be calculated by using the following equation:

$$C_s = \frac{It}{\Delta V} \quad (1)$$

where C_s is the specific capacitance (F g^{-1}) of the $Co_2P_2O_7$ electrode, I donates the discharge current (A g^{-1}), t is the discharging time (s), and ΔV is the discharge potential interval (V). Another important parameter, coulombic efficiency (η) can be evaluated from the eqn (2), where t_D and t_C are the time for galvanostatic discharging and charging, respectively.

$$\eta = \frac{t_D}{t_C} \times 100\% \quad (2)$$

The EIS "small-signal" capacitance of the $Co_2P_2O_7$ electrode can be calculated from the imaginary component of the impedance by using the equation:

$$C = \frac{1}{-2\pi f Z'' m} \quad (3)$$

where C is the EIS signal capacitance, f the frequency, m the mass of electroactive material, and Z'' the imaginary component of impedance at frequency ($f = 0.01$ Hz).

Results and discussion

After careful examination of the XRD patterns shown in Fig. 1b, it is way to find the successful transformation of the sodium hydrogen phosphate hydrate into the $Na_2H_2P_2O_7$ phase after calcination at 210 °C for 16 h. During the calcination, the glycidyl and polymerization of the $H_2PO_4^-$ occurred, as a consequence, the sodium hydrogen phosphate hydrate was completely converted into a new $Na_2H_2P_2O_7$ phase. With the

further completion of precipitation reaction between Co^{2+} and $P_2O_7^{4-}$ in the acidic media of pH = 4.14, the resultant light purple $Co_2P_2O_7$ was finally obtained (the inset in Fig. 2).

The crystalline structure of the as-synthesized $Co_2P_2O_7$ sample was further determined by XRD technique and the representative wide-angle diffraction pattern is shown in Fig. 2. The well-defined diffraction peaks, including not only the peak position, but their relative intensities, can be clearly observed, and successfully indexed to the typical reflections of the monoclinic $Co_2P_2O_7$ crystalline structure (JCPDS no. 49-1091) with a space group of $P21/c(14)$ and cell parameters of $a = 8.924$, $b = 8.366$, and $c = 9.016$, respectively. Moreover, no other discernable diffraction reflections corresponding to any other impurities can be found, indicating the high purity of the resultant $Co_2P_2O_7$ sample.

Fig. 3a and b show the typical FESEM images of the $Co_2P_2O_7$ NRs. Evidently, a large scale of 1D NRs, with ~90–200 nm in length and ~25 nm in diameter, are obtained under this condition. Interestingly, without the use of CH_3COONH_4 during the synthesis, consequently, just some $Co_2P_2O_7$ nanosheets (NSs) were evident (Fig. S1, ESI†). The pH of the solution with the absence of CH_3COONH_4 is 4.33, higher than that with the CH_3COONH_4, that is, the micro-architecture of the $Co_2P_2O_7$ samples should be influenced by the pH of the solution greatly.

To identify its microstructure more clearly, TEM and HRTEM was further performed. As seen in Fig. 4a and b, uniform NR-like morphology of the $Co_2P_2O_7$ sample is evidently exhibited, similar to the FESEM observations in Fig. 3. The SAED pattern (the inset in (b)) detected from a sampling area covering a collection of several NRs, demonstrates well-defined diffraction rings, confirming the polycrystalline nature of the as-prepared $Co_2P_2O_7$ NRs, which can be further supported by the obviously resolved lattice fringes observed in the HRTEM image (Fig. 4c). The EDAX (Fig. 4d) shows that the molar ratio of Co to P is ~0.97 in the product, very close to the stoichiometric ratio in the $Co_2P_2O_7$ compound.

Next, to evaluate the supercapacitive performance of the present $Co_2P_2O_7$ NRs, CV test was first carried out in 3 M KOH aqueous solution. Fig. 5 shows the typical CV curves of the 1D NR electrode at various scan rates ranged from 2 to 10 mV s^{-1}. Obviously, the electrochemical response currents of these CV curves on the positive sweeps are nearly mirror-image symmetric to their corresponding counterparts on the negative

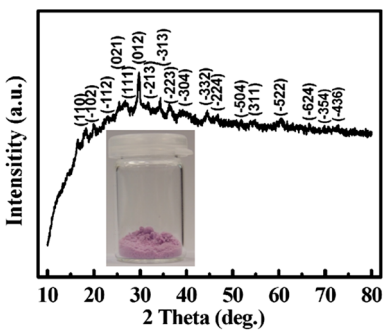

Fig. 2 Typical XRD pattern of the as-synthesized $Co_2P_2O_7$ product.

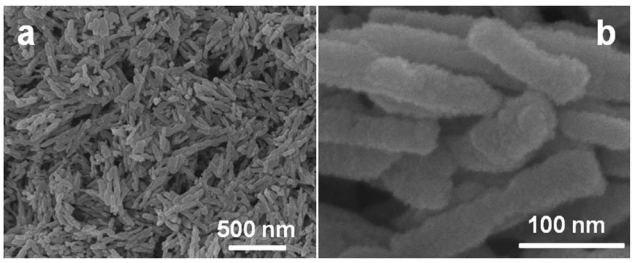

Fig. 3 FESEM images with different magnifications of the $Co_2P_2O_7$ NRs.

sweeps with respect to the zero-current line, and rapid current response on voltage reversal occurs at each end potential. The current subsequently increases while the CV shape almost keeps the same with the increase of the scan rates, which indicates good electrochemical capacitance of the unique $Co_2P_2O_7$ electrode. Strikingly, two pairs of redox peaks within −0.2–0.5 V (*vs.* SCE), which reveals that the distinguished capacitive characteristics are mainly governed by Faradaic redox reactions taking place on and/or near the surface of the 1D NR electrode, are visible over the entire range of scan rates.

Of particular note, the observed potentials for electrochemical oxidation and reduction processes, shown in CV curves presented here, greatly resemble that of the electroactive $Co(OH)_2$ in KOH solution, as reported before.[15–17] As a result, we assume that the electrochemical redox energy storage mechanism of the $Co_2P_2O_7$ electrode in KOH aqueous electrolyte should be attributed to the electrochemical inter-transition of multi-valence Co species, similar to that of $Co(OH)_2$ in alkaline electrolytes,[15–17] according to the following two expressions ((4) and (5)).

$$Co_2P_2O_7 + 2OH^- \leftrightarrow Co_2(OH)_2P_2O_7 + 2e^- \quad (4)$$

$$Co_2(OH)_2P_2O_7 + 2OH^- \leftrightarrow Co_2O_2P_2O_7 + 2H_2O + 2e^- \quad (5)$$

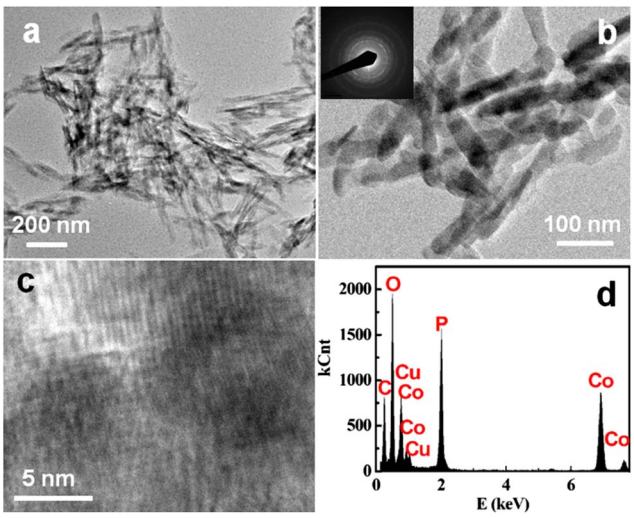

Fig. 4 TEM images (a, and b), SAED pattern (the inset in panel (b)), HRTEM image (c), and EDAX (d) of the as-obtained $Co_2P_2O_7$ NRs.

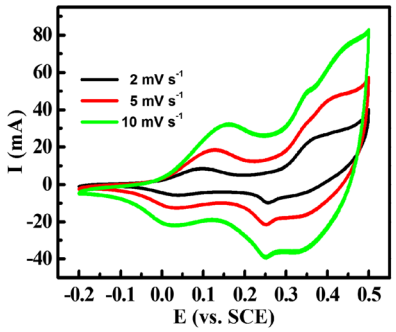

Fig. 5 CV curves of the $Co_2P_2O_7$ NR electrode at different scan rates.

Specifically, the two separated oxidation peaks positioned around 0.15 and 0.4 V (*vs.* SCE), respectively, correspond to a two-step oxidation of the Co species in the unique pyrophosphate, *i.e.*, from $Co(II)_2P_2O_7$ to $Co(III)(OH)_2P_2O_7$, and then to $Co(IV)_2O_2P_2O_7$. And the other two reductive peaks centring at ~0.25 and ~0.02 V (*vs.* SCE) are consequently related to the corresponding reverse processes. Of particular note, such a feature was not reported previously for the $Co_2P_2O_7$ nano/microstructures,[9,10] where only a pair of redox peaks were observed for the $Co_2P_2O_7$ electrodes. This difference should be ascribed to the unique 1D nanoscale NR architecture of the as-obtained $Co_2P_2O_7$ sample, which endows facile electron transport among the Co species with different valences, and high electrochemical activity.

It is well accepted that the galvanostatic charge–discharge examination is an efficient technique for estimating the SCs of electrodes. Fig. 6a shows the constant current charge–discharge plots of the $Co_2P_2O_7$ NR electrode at a series of mass-normalized currents as indicated over a potential window span ranged from −0.1 to 0.45 V (*vs.* SCE). The observation of nearly symmetric potential–time curves at all current densities implies the high charge–discharge coulombic efficiency and low polarization of the unique 1D NR electrode in KOH aqueous solution. And the nonlinear charge–discharge curves further verifies the pseudocapacitive nature of the $Co_2P_2O_7$ electrode. The relationship between the calculated SCs and current density is depicted in Fig. 6b. Attractively, the unique 1D NR electrode exhibits remarkable pseudocapacitances of 483, 476, 465, 450, 446, 432, 418 and 402 F g^{-1} at current densities of 1, 2, 3, 4, 5, 6, 8 and 10 A g^{-1}, respectively, suggesting that ~83% of the SC is still retained when the charge–discharge rate is increased from 1 to 10 A g^{-1}, which is even better than that of the $Co_2P_2O_7$ NS electrode (Fig. S2, ESI†). Specifically, as for the $Co_2P_2O_7$ NS electrode, pseudocapacitances of 456 and 353 F g^{-1} are just obtained at current density of 1 and 10 A g^{-1}, respectively, that is, ~77% of the SC retention is observed when the charge–discharge rate is up to 10 A g^{-1}. Additionally, it is noteworthy of noting that the intriguing electrochemical performance of the 1D NR electrode can be comparable to some RuO_2-based electrodes,[18,19] and even better than other $Co_2P_2O_7$ electrodes,[9,10] and some electroactive Co-based electrodes, such as, $NH_4CoPO_4 \cdot H_2O$[20] and Co-functionalized TiO_2 nanotubes.[21]

The long-term cycling stability and high coulombic efficiency of electrode materials are also critical requirements for practical ECs application. Fig. 7a depicts the plots of the SCs and coulombic efficiency as a function of the cycle number at 6 A g^{-1} for up to 3000 cycles. It can be detected that the SC retention of the NR electrode gradually reduces, whereas the SC degradation is still ~10% over continuous 3000 cycles, indicating its stable long-term cycling ability at large current density. And the possible reasons for the SC degradation should be related to the ohmic polarization and somewhat structural instability of the 1D $Co_2P_2O_7$ NR electrode during continuous charge–discharge cycles at large current density. Moreover, the coulombic efficiency (the inset in (a)) keeps at above 99% without noticeable decrease during cycling. Cycling property of the $Co_2P_2O_7$ NR electrode at progressively increased current density was further recorded in Fig. 7b. Clearly, the NR electrode exhibits stable SCs at each current density even suffering from sudden changes of the current delivery. After 1300 times of continuous cycling at varying current densities, the current is turned back to 1 A g^{-1} once again. Under this condition, still a SC of 470 F g^{-1} can be remained and maintained for another 700 cycles without obvious decrease. The electrochemical data mentioned above highlights the remarkable merits of the $Co_2P_2O_7$ NR electrode to meet the requirements of both long cycle lifetime and large SCs at high rates, which should be attributed to the good electronic conductivity and satisfactory charge transfer resistance of the 1D $Co_2P_2O_7$ NRs with rich electroactive sites.

As observed in the EIS data (Fig. 8), the good fitting indicates that the equivalent-circuit model (the inset) reasonably

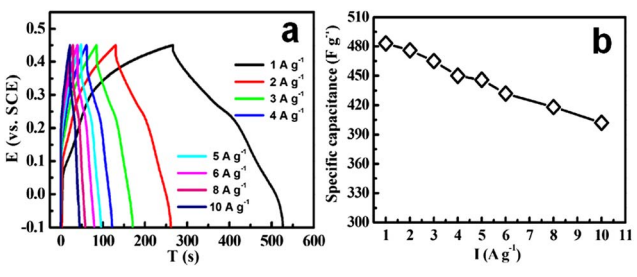

Fig. 6 CP plots (a), and SCs as a function of current densities (b) of the $Co_2P_2O_7$ NR electrode.

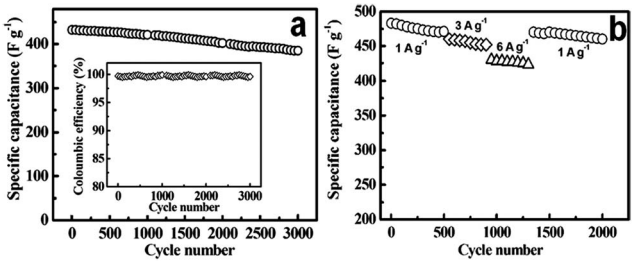

Fig. 7 Cycling life (a) and coulombic efficiency (the inset in panel (a)) at 6 A g^{-1}, and cycling performance at various current densities of the as-synthesized 1D $Co_2P_2O_7$ NR electrode.

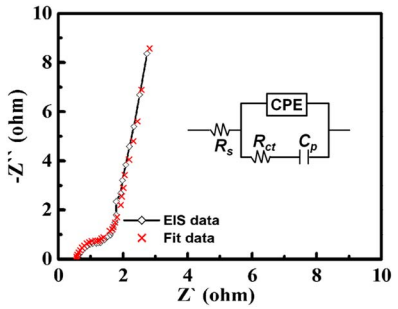

Fig. 8 EIS (0.3 V *vs.* SCE) and the fitting equivalent-circuit model (the inset) of the as-synthesized $Co_2P_2O_7$ NR electrode.

represents the electrochemical processes occurring in the unique 1D $Co_2P_2O_7$ NR electrode. Commonly, the intersection of the EIS plot at the *X*-axis represents solution resistance (R_s), which includes the following three terms:[22] the resistance of the KOH aqueous solution, the intrinsic resistance of the electroactive material itself, and the contact resistance at the interface between electroactive materials and current collector. According to the fitting data, the R_s of the as-synthesized $Co_2P_2O_7$ is ~0.55 Ω, revealing its good electronic conductivity. And at the high-medium frequency region, a semicircle can be found and its diameter stands for the charge transfer resistance (R_{ct}) in the electrochemical process, which is approximated to ~0.7 Ω, which means the low charge transfer resistance during the redox reaction for electrochemical energy storage. In addition, in the low frequency region, the slope of the impedance plot almost tends to a vertical asymptote, indicating the good electrochemical capacitance of the 1D $Co_2P_2O_7$ NR electrode in the KOH aqueous solution. Accordingly, the EIS "small-signal" capacitance of the unique $Co_2P_2O_7$ NR electrode can be calculated as ~389 F g^{-1} ($f = 0.01$ Hz) from the imaginary component of the EIS data.

Conclusions

In summary, we have established a facile but efficient one-step strategy to synthesize 1D $Co_2P_2O_7$ NRs at room temperature, and first applied it as a novel pseudocapacitive electrode for high-performance ECs. Benefiting from the intriguing 1D NR feature, the as-fabricated $Co_2P_2O_7$ NR electrode delivered excellent SCs, and stabilized cycling behaviour coupled with high coulombic efficiency at high rates in 3 M KOH aqueous solution. More significantly, the intrinsic electrochemical energy-storage mechanism of the $Co_2P_2O_7$ NR electrode in alkaline KOH aqueous media was tentatively introduced. Furthermore, the strategy we developed here prevented the high-temperature calcination, and provided a universal, efficient and scale-up approach even to synthesize other pyrophosphates ($M_2P_2O_7$, M = Ni, Mn, Cu, *etc.*) with desirable electrochemical performance for ECs. Herein, a brand-new way is now open for future development of other low-cost pseudocapacitive materials for next-generation ECs.

Acknowledgements

This work was supported by the National Natural Science Foundation of China (no. 51202004), and the Natural Science Foundation of Anhui Province (KJ2013A051).

Notes and references

1 P. Simon and Y. Gogosti, *Nat. Mater.*, 2008, **7**, 845.
2 B. E. Conway, *Electrochemical Supercapacitors: Scientific Fundamentals and Technological Applications*, Plenum, New York, 1999, ch. 15.
3 Q. Lu, J. G. G. Chen and J. Q. Xiao, *Angew. Chem., Int. Ed.*, 2013, **52**, 2.
4 W. Sugimoto, H. Iwata, Y. Yasunage, Y. Murakami and Y. Takasu, *Angew. Chem., Int. Ed.*, 2003, **42**, 4092.
5 C. Z. Yuan, L. Chen, B. Gao, L. H. Su and X. G. Zhang, *J. Mater. Chem.*, 2009, **19**, 246.
6 H. Pang, Z. Z. Yan, W. Q. Wang, Y. Y. Wei, X. X. Li, J. Li, J. Chen, J. S. Zhang and H. H. Zheng, *Int. J. Electrochem. Sci.*, 2012, **7**, 12340.
7 S. I. Nishimura, M. Nakamura, R. Natsui and A. Yamada, *J. Am. Chem. Soc.*, 2010, **132**, 13596.
8 R. A. Shakoor, H. Kim, W. Cho, S. Y. Lim, H. Song, J. W. Lee, J. K. Kang, Y. T. Kim, Y. Jung and J. W. Choi, *J. Am. Chem. Soc.*, 2012, **134**, 11740.
9 X. J. Wang, Z. Z. Yan, H. Pang, W. Q. Wang, G. C. Li, Y. H. Ma, H. Zhang, X. X. Li and J. Chen, *Int. J. Electrochem. Sci.*, 2013, **8**, 3768.
10 H. Pang, Z. Z. Yan, Y. H. Ma, G. C. Li, J. Chen, J. S. Zhang, W. M. Du and S. J. Li, *J. Solid State Electrochem.*, 2013, **17**, 1383.
11 H. Wen, M. H. Cao, G. B. Sun, W. G. Xu, D. Wang, X. Q. Zhang and C. W. Hu, *J. Phys. Chem. C*, 2008, **112**, 15948.
12 J. B. Forsyth, C. Wilkinson, S. Paster and B. M. Wanklyn, *J. Phys.: Condens. Matter*, 1989, **1**, 169.
13 H. Jiang, T. Zhao, J. Ma, C. Y. Yan and C. Z. Li, *Chem. Commun.*, 2011, **47**, 1264.
14 A. L. M. Reddy, M. M. Shaijumon, S. R. Gowda and P. M. Ajayan, *Nano Lett.*, 2009, **9**, 1002.
15 J. K. Chang, C. M. Wu and I. W. Sun, *J. Mater. Chem.*, 2010, **20**, 3729.
16 C. Z. Yuan, X. G. Zhang, B. Gao and J. Li, *Mater. Chem. Phys.*, 2007, **101**, 148.
17 C. Z. Yuan, L. R. Hou, L. F. Shen, D. K. Li, F. Zhang, C. G. Fan, J. M. Li and X. G. Zhang, *Electrochim. Acta*, 2010, **56**, 115.
18 C. C. Hu, K. H. Chang and C. C. Wang, *Electrochim. Acta*, 2007, **52**, 4411.
19 C. C. Hu, C. W. Wang, T. H. Wu and K. H. Chang, *Electrochim. Acta*, 2012, **85**, 90.
20 H. Pang, Z. Z. Yan, W. Q. Wang, J. Chen, J. S. Zhang and H. H. Zheng, *Nanoscale*, 2012, **4**, 5946.
21 L. R. Hou, C. Z. Yuan, D. K. Li, L. Yang, L. F. Shen and X. G. Zhang, *Mater. Lett.*, 2011, **65**, 2632.
22 C. Z. Yuan, X. G. Zhang, Q. F. Wu and B. Gao, *Solid State Ionics*, 2006, **177**, 1237.

